



A Journal of



Accepted Article

Title: N- Doped Carbon Wrapped Polyoxometalate Derived from POM-IL Hybrid: A Heterogeneous Catalyst for the Synthesis of Coumarin Derivatives under Solvent-Free Conditions

Authors: Meenakshi Ramalingam, Chandhru Mani, Sundar Manickam, and Kutti Rani Srinivasalu

This manuscript has been accepted after peer review and appears as an Accepted Article online prior to editing, proofing, and formal publication of the final Version of Record (VoR). This work is currently citable by using the Digital Object Identifier (DOI) given below. The VoR will be published online in Early View as soon as possible and may be different to this Accepted Article as a result of editing. Readers should obtain the VoR from the journal website shown below when it is published to ensure accuracy of information. The authors are responsible for the content of this Accepted Article.

To be cited as: *Eur. J. Inorg. Chem.* 10.1002/ejic.201900010

Link to VoR: <http://dx.doi.org/10.1002/ejic.201900010>

WILEY-VCH

N - Doped Carbon Wrapped Polyoxometalate Derived from POM-IL Hybrid: A Heterogeneous Catalyst for the Synthesis of Coumarin Derivatives under Solvent-Free Conditions

Meenakshi Ramalingam,^[a] Chandhru Mani,^[a] Sundar Manickam,^{*[b]} Kutti Rani Srinivasalu^{*[a]}

Abstract: Vanadium substituted Keggin type polyoxometalate loaded N-doped carbon was prepared from polyoxometalate ionic liquid hybrid by carbonization process. The decomposition of organic part generates various functional groups leaving polyoxometalate part intact. The catalyst was characterized by elemental analysis, FTIR, MAS ¹³C NMR, XPS and electron microscopy studies. The presence of carboxylic acids, aromatic and hetero-aromatic groups in the catalyst was confirmed by ¹³C NMR. The high resolution C1s and O1s XPS analysis further confirmed the presence of these groups. Various oxidation states of nitrogen were confirmed by deconvoluted N1s XPS spectra. Pyridine adsorption study confirms the presence of Bronsted and Lewis acid sites in the catalyst. Layered structure of the catalyst was confirmed by HR TEM analysis. The hybrid material displayed excellent catalytic activity towards the synthesis of coumarin derivatives under solvent-free conditions.

Introduction

Polyoxometalates (POMs) are nano sized metal oxide clusters of late transition metal ions with acidic and redox properties^[1]. The acidic and redox properties of POMs are easily tuned by varying the hetero or addenda atoms under optimized pH conditions. The structural multiplicity of these materials makes them attractive catalysts for various organic transformations like, epoxidations, esterification, condensation and oxidation reactions. Although, polyoxometalates are excellent catalyst for various organic reactions, their catalytic activities are restricted due to their formation of secondary aggregates in water. Moreover, the recovery and reusability of the catalysts are highly questionable as most of the polyoxometalates are highly water soluble. In order to overcome these obstacles, heterogenization of polyoxometalates on porous solids, surface modified solids etc. leads to an increase in its specific surface area and hence an increase in the catalytic activity^[2]. Also, the easy recovery and better reusability of heterogenized polyoxometalates makes them efficient catalysts for many liquid phase organic reactions.

In recent years, carbonaceous materials produced by hydrothermal carbonization (HTC) are found to be a versatile and efficient support for various organic transformations. Su et. al., reported the N- functionalized onion-like carbon (NOLC) supported H₃PW₁₂O₄₀ as an effective catalyst for ester hydrolysis^[3]. Zhang et. al., reported that the low loading (5-15%) of H₃PW₁₂O₄₀ in NOLC are efficient oxidative esterification catalyst. The better dispersion of the catalyst increases the

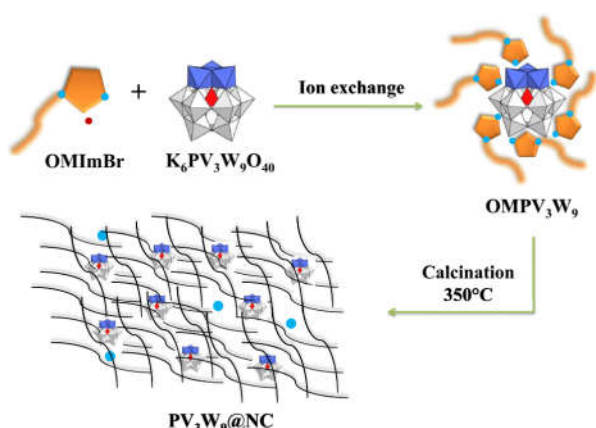
efficiency and reusability^[4]. Vanadium substituted phosphomolybdate supported on to carbon derived from potato was reported by Rafiee et.al. The material was found to be excellent catalyst for oxidative desulfurization with recyclability upto 4 cycles^[5]. Co-POM supported mesoporous carbon nitride was found to be efficient water oxidation catalyst than conventional Co-based oxidation catalyst^[6]. The high surface area of the catalyst enhances the dispersion of Co-POM and also prevents the deactivation. Wang et. al., reported new hybrid material composed of POM-IL hybrid and N-doped mesoporous carbon^[7]. The hybrid material showed good catalytic activity towards liquid phase hydroxylation of benzene. Mo₂C encapsulated N-doped carbon prepared by carbonization of polyoxometalate exchanged ionic copolymer was reported by Leng et. al. The catalyst displayed good catalytic activity on dehydrogenation of benzyl alcohols to yield selective aldehydes. Recently, the same group reported the Mo₂N nanoparticles embedded in nitrogen carbon matrix derived from ionic liquids-POM hybrids found to be an efficient catalyst for the condensation of aldehydes and amines^[8].

Coumarin is a naturally occurring benzopyrone class of compounds predominantly found in Rutaceae, Umbelliferae, Clusiaceae, Guttiferae families. As they are found in natural sources, they do possess various biochemical activities like antimicrobial, anticancer, anti-HIV, anticoagulants and antioxidant^[9]. Moreover, coumarin derivatives are widely used in various industries like food, pharmaceuticals, cosmetics^[10]. Since they show high blue-green fluorescence under UV radiations, they are used as tunable laser dyes in optics^[11]. The well known protocol for the synthesis of coumarins is Pechmann condensation. The condensation involves the reaction between phenols and active methylene compounds in presence of Bronsted or Lewis acid catalysts. As most of the heteropoly acids are Bronsted acids, Keggin type POM, H₃PMo₁₂O₄₀, H₃PW₁₂O₄₀, their ammonium salts and silica supported have been used as a catalyst for the synthesis of coumarin^[12]. The Wells-Dawson catalyst H₆P₂W₁₈O₆₂.24H₂O^[13] and silica supported^[14] was reported as an efficient catalyst for the coumarin synthesis. Heeravi et.al., compared the catalytic activity of various heteropoly acids and found Pressylar type POM was efficient in terms of high yields and shorter reaction time^[15]. The same group reported the synthesis of 3-carboxylic acid and 3-acetyl coumarins by the condensation of o-hydroxy benzaldehydes and malonic acids^[16]. Huang et. al., reported the H₃PW₁₂O₄₀ supported polyvinylpyrrolidone as a effective catalyst for the synthesis of coumarin derivatives^[17]. The supported catalyst showed better conversion and better recyclability. Ranga Rao et.al., reported the synthesis of derivatives of coumarin catalyzed by H₃PW₁₂O₄₀ modified SBA-15 under microwave condition^[18].

Herein, we synthesized N-doped carbon wrapped polyoxometalate by hydrothermal method using methyl octyl imidazolium trivanado phosphotungstate hybrid material as precursor. The catalytic activity of prepared catalyst was studied by condensation of resorcinol and ethyl acetoacetate under solvent free condition as model reaction.

[a] Department of chemistry, B.S. Abdur Rahman Crescent Institute of Science and Technology, Seethakathi Estate, Vandalur, Chennai, Tamil Nadu 600048, India.
E-mail: skrani@bsauniv.ac.in
<http://www.bsauniv.ac.in/mode/faculty/action/details/name/225-Dr-S-KUTTI-RANI>

[b] Research, Science Academy of India, Madambakkam, Chennai, Tamil Nadu 603 202, India
E-mail: sundarchemus@yahoo.com

Scheme 1: Schematic representation for the preparation of PV₃W₉@NC

Results and Discussion

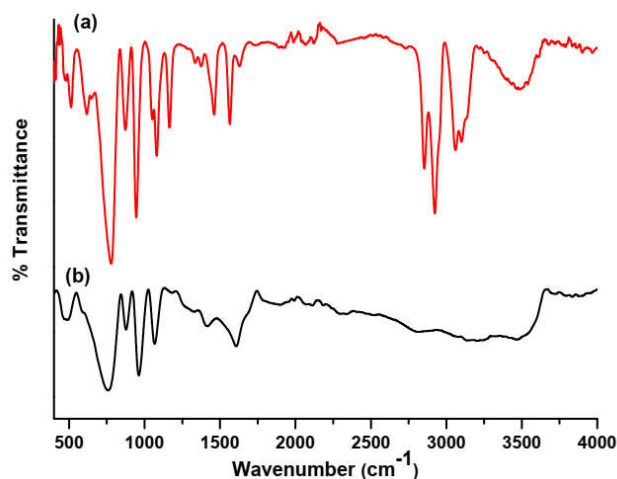
Polyoxometalate wrapped N-doped carbon was prepared using two step procedure as illustrated in the Scheme 1. In the first step, the exchange of potassium ions in PV₃W₉O₄₀ by methyl octyl imidazolium cations leads to the formation of organic inorganic hybrid material. The material will be designated hereafter as OMPV₃W₉ throughout the manuscript. The complete exchange of potassium ions by imidazolium cations was successful as evidenced from elemental analysis (Table 1). The as-prepared organic inorganic hybrid was calcined at 350°C under air atmosphere resulting in the formation of polyoxometalate encapsulated N-doped carbon hybrid (PV₃W₉@NC) as a black material. From Table 1, it is evident that the percentage of carbon, hydrogen and nitrogen content decreases, mainly due to the carbonization of organic moiety leading to the formation of oxy-functionalized groups.

Table 1. Elemental analysis of OMPV₃W₉ and PV₃W₉@NC

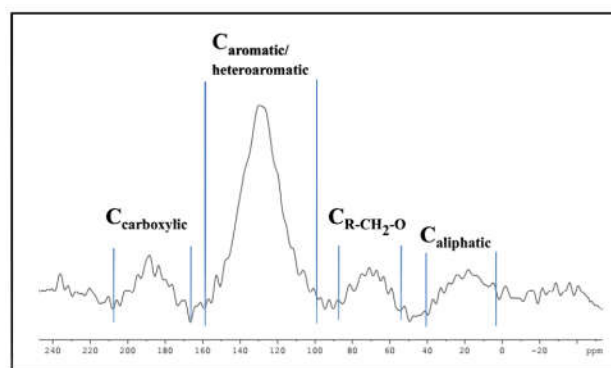
| S. No | Compounds | % C (calc) | % H (calc) | % N (calc) |
|-------|------------------------------------|------------------|----------------|---------------|
| 1.0 | OMPV ₃ W ₉ | 23.14 (23.69) | 3.74 (3.81) | 4.31 (4.6) |
| 2.0 | PV ₃ W ₉ @NC | 5.62 | 1.17 | 1.41 |

FTIR spectra of OMPV₃W₉ (Figure 1a) shows intense and multiple characteristic vibrational frequencies of both organic and inorganic moieties. It can be observed that vibrations of organic functionalities are observed in the region above 1500cm⁻¹ while the metal-oxygen stretching vibrations of [PV₃W₉O₄₀]⁶⁻ anion are usually observed in the region of 700-1200 cm⁻¹. The IR spectrum of OMPV₃W₉ showed vibrations at 1079 cm⁻¹, 1051 cm⁻¹, 944 cm⁻¹, 872 cm⁻¹ and 778 cm⁻¹ which corresponds to the ν_{as}(V_{crowm}-O_t), ν_{sym}(V_{crowm}-O_t), ν_{as}(W-O_t), ν_{as}(W-O_c-W) and ν_{as}(W-O_e-W) respectively.^[19] The stretching vibrations of octyl methyl imidazolium groups was found in the region 2800 - 3200 cm⁻¹. The octyl C-H group stretching vibrations are observed at 2922 and 2853 cm⁻¹ while imidazolium =C-H stretching vibrations are seen at 3060 and 3100 cm⁻¹. The carbonization of

OMPV₃W₉ leads to the structural deformation in the organic moiety. This can be easily identified by the decrease in intensities of vibrational frequencies (Figure 1b). The shoulder peak at 1700cm⁻¹ and also a broad peak at 3500cm⁻¹ can be attributed to the presence of carboxylic acid groups formed due to oxidation of alkyl chains during calcination. From Figure 1b it is observed that the characteristic peaks of PV₃W₉O₄₀ remains unaltered.

Figure 1. FTIR spectra of (a) OMPV₃W₉; (b) PV₃W₉@NC

The chemical environment of carbon moiety around PV₃W₉ polyoxometalate after carbonization was identified using ¹³C MAS NMR. Usually, the imidazolium and octyl groups of the OMPV₃W₉ resonate at 130 and 50 ppm respectively. As shown in Figure 2, the spectrum of PV₃W₉@NC shows common functional groups as broad peaks at 190, 129, 75 and 20ppm which indicate the formation of new functionalities after carbonization. The resonant peak at 190ppm is assigned to carboxylic acid groups. The high intense peak centered at 129ppm corresponds to the formation of non-oxygenated sp² hybridized carbons of large aromatic networks with heteroatom. The sp³ carbon bonded to heteroatoms resonates between 50 - 90 ppm while peak resonating in the region 0 - 40ppm is due to sp³ carbon bonded to aromatics and heteroatomics^[20]. From the ¹³C MAS NMR spectrum it is inferred that decomposition of alkyl chain leads to the formation of aromatic systems with oxygenated carbon species along with carboxylic acid group.

Figure 2. ¹³C MAS solid state NMR spectrum of PV₃W₉@NC after carbonization at 350°C

XPS analysis was performed to probe the nature and oxidation states of elements on the surface of the catalyst. The survey scan spectrum of the $PV_3W_9@NC$ is shown in Figure 3a. The high resolution of core level C1s spectrum (Figure 3b) is deconvoluted into 4 peaks. The binding energy at 284.65 eV attributed to C-C/C=C and 285.34 eV assigned to sp^2 C-N bonding in heteroaromatic moiety [21]. The higher binding energy peak at 286.43 eV and 288.38 eV corresponding to the carbon bonded to hydroxyl groups and carboxylic acid groups respectively [22]. Upon deconvolution of N1s high resolution spectra, four peaks were observed at 397.08, 399.08, 401.08 and 403.08 eV (Figure 3c) and they are attributed to pyridinic N, pyrrolic N, graphitic N and pyridinic-N-oxide respectively [23]. The core level O1s spectrum (Figure 3d) has been deconvoluted into four peaks: 530.27, 531.41, 532.56, and 534.08 eV and they are associated with M-O bonds, carbonyl C=O, C-OH and COOH bonds respectively.

The surface morphology of the $OMPV_3W_9$ and $PV_3W_9@NC$ was characterized by FESEM and the representative micrographs are shown in Figure 4. The SEM micrograph of the $OMPV_3W_9$ (Figure 4a) shows the clusters of cuboidal particles with sharp edges. The octyl imidazolium groups encapsulating the polyoxometalate self assemble to form cuboidal like structure. After carbonization, the complete disintegration of ordered structure leading to the formation of irregular nano clusters with different particle sizes could be observed (Figure 4b). The high resolution TEM images of $PV_3W_9@NC$ (Figure 5a, b) shows linearly ordered polyoxometalate anion (dark area) encapsulated by carbon layers (grey area).

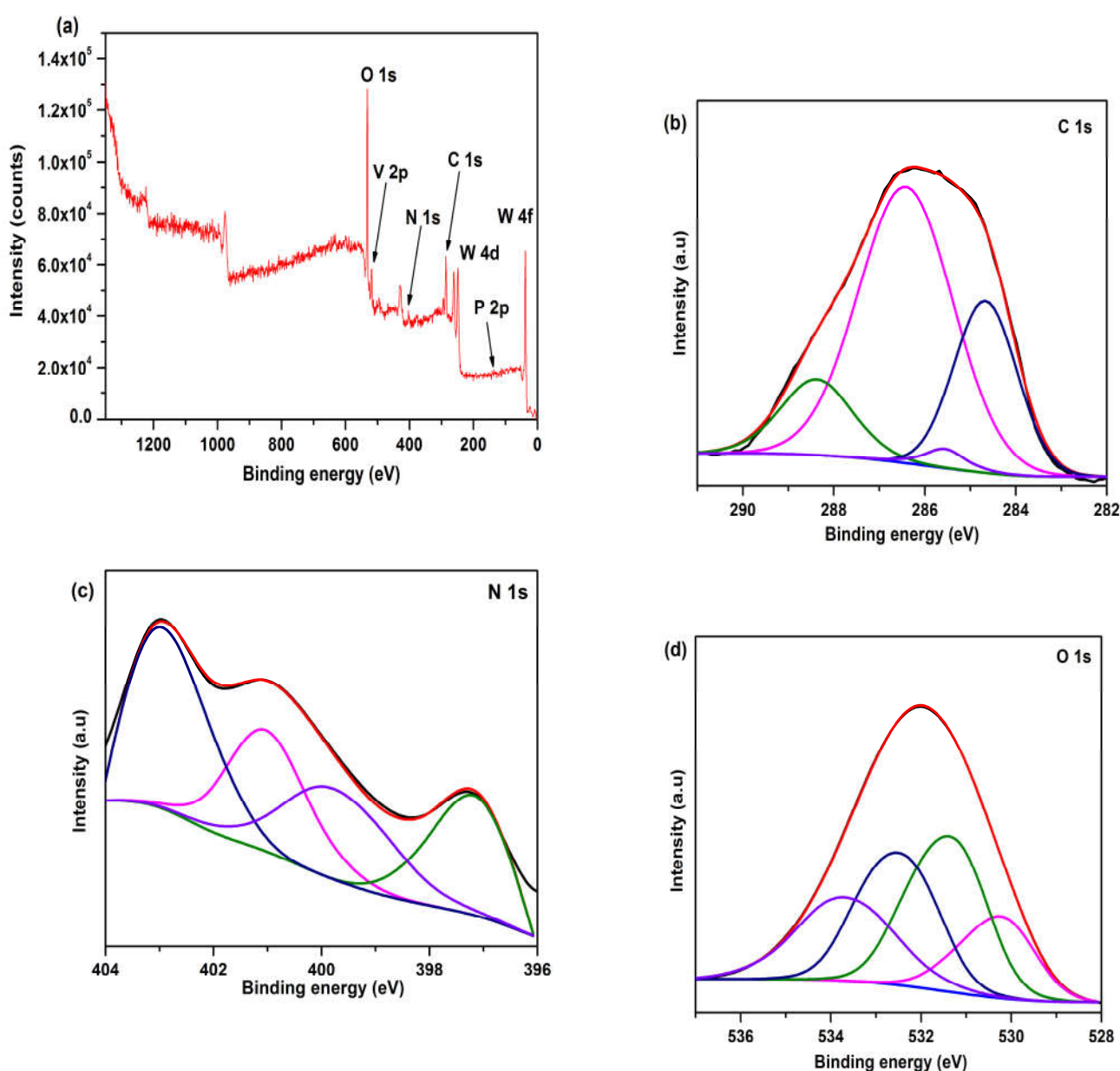


Figure 3: XPS survey spectrum of (a) $PV_3W_9@NC$, (b) high resolution XPS of C1s, (c) N1s and (d) O1s

Furthermore, pyridine adsorption study was performed to confirm the nature of acidic sites in the catalyst. Figure 6 showed the peaks at 1632, 1606, 1532, 1480 and 1445 cm^{-1} . The stretching vibrations of pyridinium ions (Brønsted acidity) are seen at 1632 and 1532 cm^{-1} while the pyridine coordinated to metal ions (Lewis acidity) are observed at 1608 and 1445 cm^{-1} . The band at 1481 cm^{-1} is the combined band of pyridine bonded to both Brønsted and Lewis acid sites [24]. Vanadium ions in the $\text{PV}_3\text{W}_9\text{O}_{40}$ anion are responsible for the Lewis acid sites and the carboxylic acid groups generated during the carbonization process are accountable for Brønsted acidity.

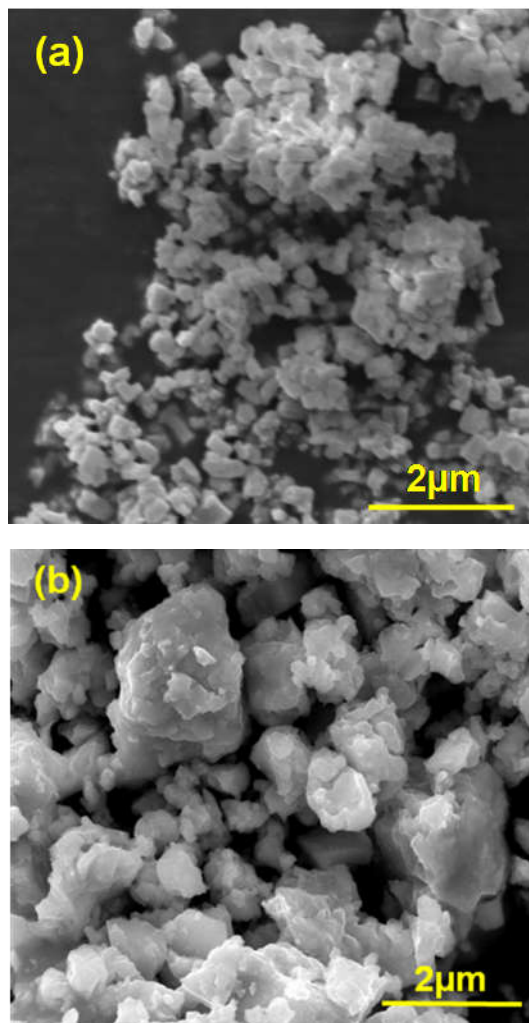


Figure 4. FESEM image of (a) OMPV_3W_9 , (b) $\text{PV}_3\text{W}_9@\text{NC}$

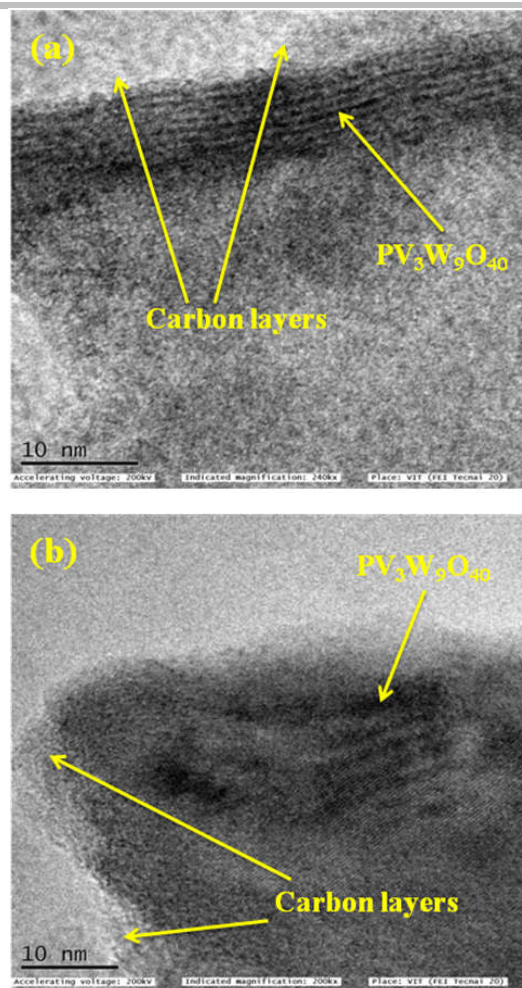


Figure 5. HRTEM image of (a) $\text{PV}_3\text{W}_9@\text{NC}$

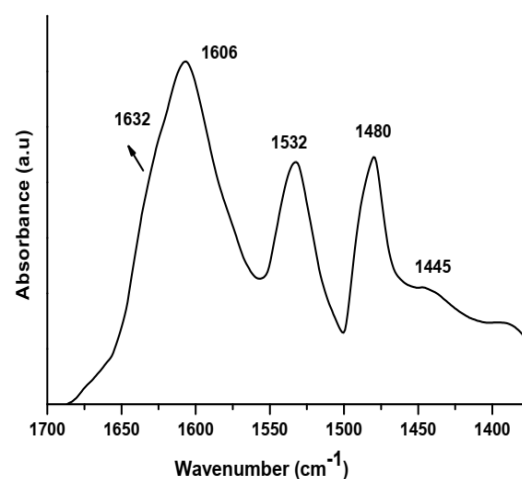


Figure 6. Pyridine-adsorption spectrum of $\text{PV}_3\text{W}_9@\text{NC}$

FULL PAPER

WILEY-VCH

Based on above characterization analysis, the possible organic moiety of the catalyst has been formulated as shown in Figure 7.

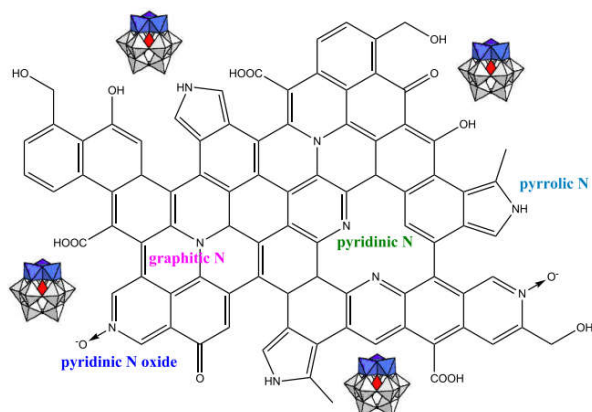


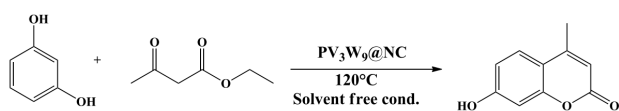
Figure 7. Possible structure of the $PV_3W_9@NC$

Table 2. Comparative study of various catalysts used for synthesis of 7-hydroxy-4-methylcoumarin^a

| S. No | Catalysts | Time (mins) | Yield (%) ^b |
|-------|----------------------------------|-------------|------------------------|
| 1.0 | $PV_3W_9@NC$ | 300 | 97 |
| 2.0 | Catalyst free | 300 | 0 |
| 3.0 | $K_6PV_3W_9$ | 300 | 15 |
| 4.0 | $OMPV_3W_9$ | 300 | 10 |
| 5.0 | $H_3PW_{12}O_{40}^c$ | 30 | 95 ^[12b] |
| 6.0 | $H_3PW_{12}O_{40} - ZrO_2^d$ | 480 | 58 ^[25] |
| 7.0 | 30% $H_3PW_{12}O_{40} - SnO_2^e$ | 120 | 78 ^[26] |
| 8.0 | $H_3PW_{12}O_{40} - PVP^f$ | 180 | 96 ^[17] |

[a] Resorcinol 2mmol, ethyl acetoacetate : resorcinol = 1.1, 0.2g of catalyst, 120°C, [b] GC yield, [c] resorcinol 1mmol, methyl acetoacetate : resorcinol = 1, 2mol% of catalyst, 130°C, [d] resorcinol 10mmol, methyl acetoacetate : resorcinol = 1.5, 0.2g of catalyst, 130°C, [e] resorcinol 10mmol, ethyl acetoacetate : resorcinol = 2, 0.1g of catalyst, 120°C, [f] resorcinol 0.1mol, ethyl acetoacetate : resorcinol = 1.3, 1g of catalyst, toluene, 100°C,

Catalytic activity



Scheme 2: synthesis of 7-hydroxy -4-methyl coumarin

The synthesis of coumarin derivatives by the condensation of resorcinol and ethyl acetoacetate was chosen as a model reaction to test the catalytic activity of the $PV_3W_9@NC$ (Scheme 2). Table 2 shows the catalytic activity of $PV_3W_9@NC$ in comparison with free phosphotungstic acid and supported catalyst. The present catalyst, $PV_3W_9@NC$ gives the high yield

of 7-hydroxy-4-methylcoumarin (97%) after 5 hrs at 120°C (Table 2, entry 1). When the same reaction was performed without the aid of catalyst no product was observed (Table 2, entry 2). Similarly, the precursor polyoxometalates; $K_6PV_3W_9$ and $OMPV_3W_9$ also gave poor yield under identical reaction conditions (Table 2, entry 3&4). These studies confirmed that the condensation reaction is mainly influenced by the carboxylic acid sites in the catalyst formed during the carbonization process. The $H_3PW_{12}O_{40}$ catalyst showed a yield of 95% coumarin in lesser reaction time (Table 2, entry 5). The phosphotungstic acid supported catalyst with high substrate to catalyst ratio (Table 2, entry 6, 7 & 8) gave variable results in terms of yield and catalyst loading. From the table 2, it is evident that $PV_3W_9@NC$ has similar activity with higher reaction times compared to that of supported catalysts.

Table 3. $PV_3W_9@NC$ catalysed synthesis of coumarin derivatives under solvent free conditions^a

| S. No | Phenol derivatives | Product | % yield ^b |
|-------|--------------------|---------|----------------------|
| 1.0 | | | 92 |
| 2.0 | | | 97 |
| 3.0 | | | 86 |
| 4.0 | | | 76 |
| 5.0 | | | 60 |
| 6.0 | | | 88 ^c |

[a] Resorcinol 2mmol, ethyl acetoacetate : resorcinol = 1.1, 0.2g of catalyst, 120°C, 5hrs, [b] GC yield, [c] catalyst reused twice.

In order to evaluate the versatility of the catalyst, substrate generality was performed using combinations of dihydroxybenzene derivatives and ethyl acetoacetate. In all the cases studied, the reaction was successful with good to excellent yields of corresponding coumarins. The results obtained are as shown in Table 3. It could be noted that resorcinol (Table 3, entry 2) gives better yield when compared to hydroquinone and catechol (Table 3, entry 3&1). It is due to the strong resonance effect of *m*-hydroxy group on the substrate. The yield is considerably low when electron releasing substituent (-CH₃) is present either in *o*- or *m*- positions to phenolic -OH groups. Steric hinderance of *o*-CH₃ results in the low conversion for 2-methyl resorcinol (Table 3, entry 4). Similar case was observed for 5-methyl resorcinol (Table 3, entry 5) where the presence of -CH₃ in meta-position decreases the rate of attack of phenolic -OH group on carbonyl group of β -keto esters [27].

As far as the mechanistic aspect of the condensation reaction is concerned, the first step is the Bronsted acid sites catalyzed transesterification reaction between resorcinol and ethyl acetoacetate followed by intramolecular hydroxyalkylation leading to the formation of cyclic intermediate. The presence of nitrogen atoms improves the basicity of the catalyst and facilitates the abstraction of protons in the final dehydration step.

The reusability study was performed to test the efficiency and robustness of the catalyst. The catalyst after the reaction was recovered by centrifugation and reused for the catalytic reaction. When compared to the fresh catalyst, the catalytic activity of the reused catalyst reduced from 97 to 88% after two runs (Table 3, entry 6). This decrease in activity could be ascribed to the deactivation of Brønsted acid sites during the subsequent runs. As the interactions between PV₃W₉ and N-doped carbon weak, there is a possibility of carbon leaching during recovery process. The FTIR of reused catalyst (Figure 8) showed most of the stretching vibrations of POMs are strong and undisturbed which indicates inorganic anion, i.e. PV₃W₉O₄₀ group are intact and stable, while broadening of peaks was observed in the organic part of the catalyst.

The efficiency and robustness of the catalyst can be improved by increasing the number of alkyl chains in the ionic liquid group's thereby increasing carbon content or minimizing the loss of organic moiety during carbonization process. On the other hand, substituting POMs with high oxidation potential to promote synergistic effects of both Brønsted and Lewis acidity

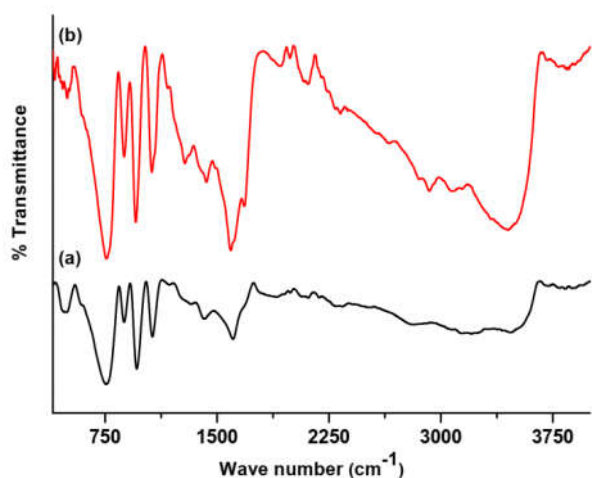


Figure 8. FTIR spectra of (a) Fresh PV₃W₉@NC (b) Reused PV₃W₉@NC

Conclusions

In conclusion, we have prepared phosphovanadotungstate loaded N doped carbon catalyst by simple metathesis followed by carbonization. The prepared catalyst was characterized by elemental analysis, FTIR and morphology studies. The structure of the catalyst was evaluated by MAS ¹³C NMR and XPS analysis. Brønsted and Lewis acid behavior was studied using pyridine adsorption analysis. The catalyst showed excellent yield for unsubstituted resorcinol while moderate yield was obtained for substituted compounds. The control experiments showed that the catalysis was mainly governed by Brønsted acid sites formed in the support during carbonization. The catalyst could be reused twice with little loss in activity.

Experimental Section

Materials and methods:

N-Methyl imidazole and 1-bromooctane were purchased from Sigma Aldrich. Sodium tungstate, phosphoric acid (85 weight %), glacial acetic acid, sodium metavanadate and potassium chloride were purchased from Merck. Dihydroxy compounds and ethyl acetoacetate were purchased from Avra chemicals and used as such without any purification. Methyl octyl imidazolium bromide, potassium trivanadium phosphotungstate, methyl octyl imidazolium trivanadotungstate hybrid were prepared as per process given in the literature. [28]

Measurements

Elemental analysis was performed using a German Elemental vario micro cube. The IR spectra of the samples were recorded in the ATR mode with a Jasco FT/IR-6300 instrument in the 4000–400 cm⁻¹ range. ¹³C solid-state MAS NMR experiments were acquired on a Bruker DPX-200 (200MHz) (7 T) spectrometer using 4 mm zirconia rotors as sample holders, spinning at MAS rate ν MAS = 14 kHz. The chemical shift reference was tetramethylsilane (TMS; δ = 0 ppm). ¹H t_1 relaxation time was set to 3 s. Proton-to-carbon CP MAS was used to enhance carbon sensitivity with a cross polarisation time equal to 1 ms. X-ray photoelectronspectra was recorded with an ESCA-3 Mark II spectrometer (VGScientific Ltd., UK) with Al-K α (1486.6 eV) radiation as the source. Spectra were referenced to the binding energy of C1s (285 eV). Scanning electron microscope images were acquired with a JEOL FESEM 6700F electron microscope. Transmission electron microscopy (TEM) was performed with a JEOL model JEM-2100 electron microscope operated at an accelerating voltage of 200 kV. The pyridine adsorption studies were performed using diffuse reflectance infrared Fourier transform (DRIFT). The catalyst was mixed with dry pyridine and excess pyridine was removed by drying the sample at 120°C under vacuum for 2hrs. After cooling the catalyst to room temperature, the FTIR was recorded for the pyridine adsorbed catalyst. The product from catalytic study was analysed using gas chromatography (Shimadzu 2014) with use of a capillary column (Rtx-5, 30 m \times 0.32 mm ID \times 1 μ m) and FID detector. Nitrogen was used as the carrier gas at a flow rate of 37.1 mL min⁻¹ and a column flow of 1.1 mL min⁻¹. The products were confirmed by GC-MS (Perkin-Elmer). A Clarus 680 chromatograph with capillary column (Elite-5MS, 30 m \times 0.25 mm ID \times 250 μ m df) connected to a Clarus 600 (EI) mass spectrometer.

Preparation of PV₃W₉@NC:

5g of methyl octyl imidazolium trivanado phosphotungstate was calcined at 350°C under air atmosphere for 1 hour. After calcination, 2.0 g of catalyst was obtained as a black solid.

Synthesis of 7-Hydroxy -4-Methyl Coumarin : General procedure

0.2g of PV₃W₉@NC catalyst was added to the reaction mixture containing resorcinol (2mmol) and ethyl acetoacetate (2.2mmol). The reaction mixture was heated to 120°C for 5hrs. After 5 hrs, 10ml chloroform was added to remove the catalyst by centrifugation. The organic layer obtained was washed with brine solution and dried using sodium sulphate. The chloroform solution was filtered and analysed for products by gas chromatography.

Acknowledgements

We would like to thank Head, Business Development & Information Management Discipline (BDIM), CSMCRI, Bhavnagar, Gujarat for MAS-¹³C NMR and elemental analysis. We thank Central facilities, SASTRA Deemed University, Thanjavur for XPS characterisation. Nanotechnology Research Centre, SRM University is gratefully acknowledged for FESEM analysis. Authors thank SAIF, B.S. Abdur Rahman Crescent Institute of Science and Technology for FTIR, pyridine adsorption and GC analysis. We thank Vellore Institute of Technology-Sofisticated Instrumental Facility lab, Chemistry Division, Vellore, for GC-MS analysis.

Keywords: N-doped carbon; polyoxometalates; coumarin; pechmann condensation; solvent-free conditions; Brønsted acid catalysis.

- [1] I. V. Kozhevnikov, *Chem. Rev* **1998**, *98*, 1–390. The entire issue is devoted to polyoxometalates.
- [2] (a) Y. Zhou, G. Chen, Z. Long, & J. Wang, *RSC Adv* **2014**, *4*, 42092-42113. (b) M.N. Timofeeva, *Appl. Catal. A. Gen.* **2003**, *256*, 19-35. (c) E. Rafiee, S. Eavani, S. *RSC Adv* **2016**, *6*, 46433-46466. (d) Y. Zhou, G. Chen, Z. Long, J. Wang, *RSC Adv* **2014**, *4*, 42092-42113.
- [3] W. Liu, W. Qi, X. Guo, X. D. Su, *Chem. Asian, J* **2016**, *11*, 491-497.
- [4] P. Huang, A. Liu, L. Kang, B. Dai, M. Zhu, J. Zhang, *ChemistrySelect*, **2017**, *2*, 4010-4015.
- [5] E. Rafiee, M. Joshaghani, P. G. S. Abadi, *J. Saud. Chem. Soc.* **2017**, *21*, 599-609.
- [6] G. Y. Lee, I. Kim, J. Lim, M. Y. Yang, D. S. Choi, Y. Gu, S. O. Kim, *J. Mater.Chem A*, **2017**, *5*, 1941-1947.
- [7] X. Cai, Q. Wang, Y. Liu, J. Xie, Z. Long, Y. Zhou, J. Wang, *ACS Sustain Chem Eng* **2016**, *4*, 4986-4996.
- [8] Y. Leng, J. Li, C. Zhang, P. Jiang, Y. Li, Y. Jiang, S. Du, *J. Mater. Chem. A* **2017**, *5*, 17580-17588. (b) Y. Li, K. Xiao, J. Li, P. Jiang, Y. Jiang, S. Du, Y. Leng, *ChemCatChem* **2018**, *10*, 4317-4323.
- [9] a) T. Smyth, V.N. Ramachandran, W. F. Smyth, *Int J Antimicrob Agents* **2009**, *33*, 421-426. b) A. Thakur, R. Singla, V. Jaitak, *Eur J Med Chem* **2015**, *101*, 476-495. c) C. Spino, M. Dodier, S. Sotheeswaran, *Bioorganic. Med. Chem. Lett.* **1998**, *8*, 3475-3478. d) J. Koch-Weser, E. M. Sellers, *N Engl J Med* **1971**, *285*, 547-558. e) I. Kostova, S. Bhatia, P. Grigorov, S. Balkansky, V. S. Parmar, A. K. Prasad, L. Saso, *Curr. Med. Chem.* **2011**, *18*, 3929-3951. f) K. C. Fylaktakidou, D. J. Hadjipavlou-Litina, K. E. Litinas, D. N. Nicolaidis, D. N. *Curr. Pharm. Des.* **2004**, *10*, 3813-3833.
- [10] a) T. Bintsis, E. Litopoulou-Tzanetaki, R. K. Robinson, *J. Sci, Food. Agr.* **2000**, *80*, 637-645. b) R. S. Keri, B. S. Sasidhar, B. M. Nagaraja, M. A. Santos, *Eur. J. Med. Chem.* **2015**, *100*, 257-269. c) J. G. Evans, I. F. Gaunt, B. G. Lake, *Food. Cosmet. Toxicol.* **1979**, *17*, 187-193.
- [11] M. Maeda, *Laser Dyes*, Academic, New York, 1994. b) X. Liu, J. M. Cole, P. G. Waddell, T. C. Lin, J. Radia, A. Zeidler, *J. Phys. Chem. A*, **2011**, *116*, 727-737.
- [12] a) R. Torviso, D. Mansilla, A. Belizán, E. Alesso, G. Moltrasio, P. Vázquez, L. Pizzio, M. Blanco C. Cáceres, *Appl. Catal. A. Gen.*, **2008**, *339*, 53-60. b) R.S. Keri, K. M. Hosamani, H. R. S. Reddy, *Catal. Lett.* **2009**, *131*, 321-327.
- [13] G. P. Romanelli, D. Bennardi, D. M. Ruiz, G. Baronetti, H. J. Thomas, J. C. Autino, *Tetrahedron Lett.*, **2004**, *45*, 8935-8939.
- [14] D. Bennardi, D. Ruiz, G. P. Romanelli, J. C. Autino, G. Baronetti, H. J. Thomas, *Lett. Org. Chem.*, **2008**, *5*, 607-615.
- [15] M. M. Heravi, M. Khorasani, F. Derikvand, H. A. Oskooie, F. F. Bamoharram, *Catal. Commun.* **2007**, *8*, 1886-1890.
- [16] M.M. Heravi, S. Sadjadi, H.A. Oskooie, R. H. Shoar, F. F. Bamoharram, *Catal. Commun.*, **2008**, *9*, 470-474
- [17] S. Li, X. Qi, B. Huang, *Catal. Today*, **2016**, *276*, 139-144.
- [18] P. H. K. Charan, G. R. Rao, *Adv. Porous. Mater*, **2015**, *2*, 192-203.
- [19] a) R. G. Finke, M. W. Droegge, P. J. Domaille, *Inorg.Chem.* **1987**, *26*, 3886–3896. b) M. J. Watras, A. V. Teplyakov, *J. Phys. Chem. B* **2005**, *109*, 8928–8934
- [20] a) C. Falco, N. Baccile, M. M. Titirici, *Green Chem*, **2011**, *13*, 3273-3281 b) N. Baccile, G. Laurent, C. Coelho, F. Babonneau, L. Zhao, & M. M. Titirici, *J. Phys. Chem C*, **2011**, *115*, 8976-8982.
- [21] a) W. Zheng, R. Tan, S. Yin, Y. Zhang, G. Zhao, Y. Chen, D. Yin, *Catal. Sci. Technol.* **2015**, *5*, 2092-2102.
- [22] F. Zhao, A. Vrajitoarea, Q. Jiang, X. Han, A. Chaudhary, A., J.O. Welch, R.B. Jackman, *Sci. Rep.* **2015**, *5*, 13771-13782.
- [23] a) M. Rana, G. Arora, U. K. Gautam, *Sci. Technol. Adv. Mater*, **2015**, *16*, 014803-14814. b) B. Grzyb, S. Gryglewicz, A. Śliwak, N. Diez, J. Machnikowski, G. Gryglewicz, *RSC Adv*, **2016**, *6*, 15782-15787. M. Inagaki, M. Toyoda, Y. Soneda, T. Morishita, *Carbon*, **2018**, *132*, 104.
- [24] B. M. Devassy, S. B. Halligudi, *J. Cat.* **2005**, *236*, 313.
- [25] S. Ghodke, U. Chudasama, *Appl. Catal. A. Gen.* **2013**, *453*, 219-226.
- [26] A. I. Ahmed, S.A. El-Hakam, M. A. Elghany, W. A. El-Yazeed, *Appl. Catal. A. Gen.* **2011**, *407*, 40-48.
- [27] (a) B. Tyagi, M.K. Mishra, R. V. Jasra, R. V. J. Mol. Catal. A: Gen, **2008**, *286*, 41-46. (b) P. Kalita, R. Kumar, microporous. Mesoporous. Meter. **2012**, *149*, 1-9.
- [28] C. Mani, M. Ramalingam, S. Manickam, K.R. Srinivasalu, E. Deivanayagam, B.I. Mohammed, *ChemistrySelect*, **2017**, *2*, 9934-9942.